Bulletin of the Seismological Society of America, 91, 3, pp. 553–560, June 2001

A Reciprocity Method for Multiple-Source Simulations

by Leo Eisner* and Robert W. Clayton

Abstract Reciprocity is applied to the situation where numerical simulations are needed for a number of source locations but relatively a few receiver positions. By invoking source-receiver reciprocity, the number of simulations can be generally reduced to three times the number of receiver positions. The procedure is illustrated for a heterogeneous medium with both single-force and double-couple sources. The numerical tests using a finite-difference implementation show that the reciprocal simulations can be performed with the same level of accuracy as the forward calculations.

Introduction

Simulations of waves in complex 3D media have shown that wave propagation in basinlike structures can cause significant variations in amplitudes, travel times, and coda of the strong ground motion (Graves, 1995; Olsen *et al.,* 1997; Wald and Graves, 1998). The usual procedure is to evolve the wave field outward from the source location to a suite of observation points, which means that one complete simulation needs to be done for each source location. For many problems such as comparing seismograms recorded for many earthquakes at a particular site, this straightforward approach can be computationally expensive. The same situation is true for iteratively calculating the source response for inverse problems.

However, with the use of three orthogonal point forces at the receiver locations and the reciprocity theorem, the number of numerical calculations can be reduced to three times the number of the receivers. Here we show a technique for calculating the Green's functions for the full elasto-dynamic equation that exploits reciprocity to reduce the number of simulations.

The property of source-receiver reciprocity has been known for a long time for the elasto-dynamic equations of motion and has been widely used in exploration seismology. Claerbout (1976), for example, shows that reciprocity is a fundamental quality of the elasto-dynamic equation. Reciprocity of the ray theoretical reflection/transmission in anisotropic medium was finally resolved by Chapman (1994), and a general proof for arbitrary media is given by Červený (2001). de Hoop and de Hoop (2000) gave an extensive overview of the application of the reciprocity in the remote sensing including a generalized theory for source inversion. There are several applications of the reciprocity theorem to the full waveform modeling in seismology. Bouchon (1976) used reciprocity to develop a technique for computation of synthetic seismograms due to sources in a strongly heterogeneous medium. Our article extends the work of Graves and Clayton (1992) who used reciprocity for acoustic modeling of path effects in 3D basin structures. Recently Graves and Wald (2000) applied elastic reciprocity to the finite-fault inversion.

In this article we shall first give a detailed proof of the reciprocity theorem with sources on the boundary of domain of interest. Then we shall discuss a numerical implementation of the reciprocity for a finite-difference method. The finite-difference method is particularly suitable for the application of reciprocity method since the whole 3D volume is calculated for each run; thus an arbitrary number of sources can be simulated in the 3D volume. Finally we shall numerically test the accuracy of the reciprocity method on several simple models.

The Reciprocity Theorem

The reciprocity theorem is proven in Aki and Richards (1980) for an elastic anisotropic continuous medium. Dahlen and Tromp (1998) generalized their proof for anelastic, piecewise continuous body. In this article we discuss in detail the boundary conditions of reciprocity theorem as needed for the reciprocity method. We extend proof of Dahlen and Tromp (1998) for source and receiver positions on the boundary of an area of interest. The basic statement of reciprocity is contained in Betti's theorem by Dahlen and Tromp (1998), who show Betti's reciprocal relation for a piecewise continuous anelastic body with total volume V bounded by surface Σ (equation 5.64 of Dahlen and Tromp [1998]):

*Present address: Schlumberger Cambridge Research, High Cross, Madingley Rd., Cambridge, CB30EL, England.

$$\int_{-\infty}^{\infty}\int_{V} s_i(\mathbf{x},\,\mathbf{x}';\,t\,-\,t')\bar{f}_i(\mathbf{x},\,\mathbf{x}';\,-t,\,t')\partial V\,dt + \int_{-\infty}^{\infty}\int_{\partial V} s_i(\mathbf{x},\,\mathbf{x}';\,t\,-\,t')\bar{t}_i(\mathbf{x},\,\mathbf{x}';\,-t,\,t')d\Sigma dt = \int_{-\infty}^{\infty}\int_{V} \bar{s}_i(\mathbf{x},\,\mathbf{x}';\,-t\,+\,t')f_i(\mathbf{x},\,\mathbf{x}';\,t,\,t')\partial V\,dt + \int_{-\infty}^{\infty}\int_{\partial V} \bar{s}_i(\mathbf{x},\,\mathbf{x}';\,-t\,+\,t')t_i(\mathbf{x},\,\mathbf{x}';\,t,\,t')d\Sigma dt. \quad (1)$$

Here $s_i(\mathbf{x}, \mathbf{x}'; t - t')$ is the ith component of the displacement vector, which is a solution of the elasto-dynamic equations.

$$\rho(\mathbf{x})\frac{\partial^2}{\partial t^2}\,s_i(\mathbf{x},\,\mathbf{x}';\,t\,-\,t') = f_i(\mathbf{x},\,\mathbf{x}';\,t\,-\,t') + \frac{\partial}{\partial x_k}\left(\int_{-\infty}^{t'} c_{iklm}(\mathbf{x},\,t'\,-\,\tau)\,\frac{\partial}{\partial x_m}\,s_l(\mathbf{x},\,\mathbf{x}';\,t\,-\,\tau)d\tau\right), \quad (2)$$

with traction condition on the surface of volume V (∂V)

$$t_i(\mathbf{x},\,\mathbf{x}';\,t\,-\,t',\,0) = g_i(\mathbf{x},\,\mathbf{x}';\,t\,-\,t',\,0) + n_j\int_{-\infty}^{t'} c_{ijkl}(\mathbf{x},\,t'\,-\,\tau)\,\frac{\partial}{\partial x_l}\,s_k(\mathbf{x},\,\mathbf{x}';\,t\,-\,\tau)\mathrm{d}\tau, \quad (3)$$

where $\mathbf{n}$ is a normal to the boundary of the volume V, $c_{ijkl}(\mathbf{x})$ is a tensor of elastic parameters, and $\rho(\mathbf{x})$ is density characterizing a medium. The vector $\mathbf{f}$ represents the body forces inside the volume V, and the vector $\mathbf{g}$ traction on the surface of the volume V. The barred variables satisfy the analogous condition

$$\rho(\mathbf{x})\frac{\partial^2}{\partial t^2}\,\bar{s}_i(\mathbf{x},\,\mathbf{x}';\,-t\,+\,t') = \bar{f}_i(\mathbf{x},\,\mathbf{x}';\,-t\,+\,t',\,0) + \frac{\partial}{\partial x_k}\left(\int_{-\infty}^{t'} c_{iklm}(\mathbf{x},\,t'\,-\,\tau)\,\frac{\partial}{\partial x_m}\,\bar{s}_l(\mathbf{x},\,\mathbf{x}';\,-t\,+\,\tau)d\tau\right), \quad (4)$$

with the analogous traction condition on ∂V

$$t_i(\mathbf{x},\,\mathbf{x}';\,-t\,+\,t',\,0) = \bar{g}_i(\mathbf{x},\,\mathbf{x}';\,-t\,+\,t',\,0) + n_j\int_{-\infty}^{t'} c_{ijkl}(\mathbf{x},\,t'\,-\,\tau)\,\frac{\partial}{\partial x_l}\,\bar{s}_k(\mathbf{x},\,\mathbf{x}';\,-t\,+\,\tau)d\tau. \quad (5)$$

To derive Betti's theorem (1), both barred and unbarred equations must satisfy continuity of the normal stresses at the discontinuities of $c_{ijkl}(\mathbf{x})$ and $\rho(\mathbf{x})$ and the forces $\mathbf{f}$ and $\bar{\mathbf{f}}$ have to be such that their contributions from time $t = \infty$ and $t = -\infty$ vanish. For an unbounded medium or a partially unbounded medium (such as a layered halfspace), the boundary conditions (3) and (5) are satisfied over the unbounded part of the medium as the left-hand side of both conditions (3) and (5) vanish (either the source at infinity does not exist or, if it does, it takes an infinite time to receive any information about its existence), and so does the right-hand side of (3) and (5) as the vector of displacement must be zero at infinity. Therefore, the traction conditions (3) and (5) act only on the boundaries at finite distance.

Now we shall make a special choice of the source and receiver for the barred and unbarred variables and derive the reciprocity of the source and receiver position. By taking $\bar{\mathbf{t}}$ to be zero at the ∂V, and $\bar{\mathbf{f}}$ impulsive,

$$\bar{\mathbf{f}}(\mathbf{x},\,\mathbf{x}';\,t,\,t') = \mathbf{e}_j\delta(\mathbf{x}'\,-\,\mathbf{x})\delta(t'\,+\,t),\ \bar{\mathbf{t}}(\mathbf{x},\,\mathbf{x}';\,t,\,t') = 0,$$

or $\bar{\mathbf{t}}$ impulsive at the ∂V, and $\bar{\mathbf{f}}$ zero everywhere in V

$$\bar{\mathbf{f}}(\mathbf{x},\,\mathbf{x}';\,t,\,t') = 0,\ \bar{\mathbf{t}}(\mathbf{x},\,\mathbf{x}',\,t,\,t') = \mathbf{e}_j\delta(\mathbf{x}'\,-\,\mathbf{x})\delta(t'\,+\,t),$$

where $\mathbf{e}_j$ is a unit vector in a direction of jth axis, and body force $\mathbf{f}$ and traction $\mathbf{t}$ are oriented along the vector $\mathbf{e}_j$. The ith component of the displacement vector $\mathbf{s}$ becomes by definition the ith component of the Green's function due to force acting along the $\mathbf{e}_j$ vector:

$$\bar{G}_{ji}(\mathbf{x},\,\mathbf{x}';\,-t\,+\,t') \equiv \bar{s}_i(\mathbf{x},\,\mathbf{x}';\,-t\,+\,t').$$

Hence, equation (1) reduces to

$$s_j(\mathbf{x},\mathbf{x}';\,t-t') = \int_{-\infty}^{\infty}\int_{V} \bar{G}_{ji}(\mathbf{x},\mathbf{x}';\,-t+t')f_i(\mathbf{x},\mathbf{x}';\,t+t',\,0)\partial V\,dt + \int_{-\infty}^{\infty}\int_{\partial V} \bar{G}_{ji}(\mathbf{x},\mathbf{x}';\,-t+t')t_i(\mathbf{x},\mathbf{x}';\,t-t',\,0)d\Sigma dt. \quad (6)$$

And further by letting $\mathbf{t}$ to be zero at the ∂V, and $\mathbf{f}$ impulsive

$$\mathbf{f}(\mathbf{x},\,\mathbf{x}',\,t,\,t') = \mathbf{e}_i\delta(\mathbf{x}\,-\,\mathbf{x}')\delta(t\,-\,t'),\ \mathbf{t}(\mathbf{x},\,\mathbf{x}',\,t,\,t') = 0,$$

or $\mathbf{t}$ impulsive at the ∂V, and $\mathbf{f}$ zero everywhere in V:

$$\mathbf{f}(\mathbf{x},\,\mathbf{x}',\,t,\,t') = 0,\ \mathbf{t}(\mathbf{x},\,\mathbf{x}',\,t,\,t') = \mathbf{e}_i\delta(\mathbf{x}\,-\,\mathbf{x}')\delta(t\,-\,t'),$$

and analogously, the jth component of the displacement vector $\mathbf{s}$ becomes by definition the jth component of the Green's function due to force acting along the $\mathbf{e}_i$ vector:

$$G_{ij}(\mathbf{x},\,\mathbf{x}';\,t\,-\,t') \equiv s_j(\mathbf{x},\,\mathbf{x}';\,t\,-\,t').$$

We obtain from (6) the reciprocal relation:

$$G_{ij}(\mathbf{x},\,\mathbf{x}',\,t\,-\,t') = \bar{G}_{ji}(\mathbf{x}',\,\mathbf{x},\,t\,-\,t'). \quad (7)$$

This proof of reciprocity is valid anywhere in the volume V or on its boundaries ∂V. Equation (7) allows the source and receiver points to be interchanged, and identical seismograms will be recorded if the sources or receivers are situated inside the volume V or on its boundary δV. The proof is valid for a solution of elasto-dynamic equation (2, 4) with

linearized attenuation represented by a stress-strain relationship

$$\sigma_{ij}(\mathbf{x},\ t)\ =\ \int_{-\infty}^{t} c_{ijkl}(\mathbf{x},\ t\ -\ \tau)\varepsilon_{kl}(\mathbf{x},\ \tau)d\tau.$$

Equation (7) can be directly applied for evaluating the elastic fields from a single force point source by placing three single force sources at the receiver site ($\mathbf{x}$) and calculating response at the source area ($\mathbf{x}'$). However, elastic fields due to a double-couple (or a single-couple, or an explosive) point source require evaluation of the derivatives of the Green's functions:

$$u_i(\mathbf{x},\ \mathbf{x}',\ t\ -\ t')\ =\ \frac{d\overline{G}_{ji}(\mathbf{x},\ \mathbf{x}',\ t\ -\ t')}{dx'_k}\ *\ M_{jk}(x',\ t')$$

where * represents time convolution over time. This equation can be evaluated by taking a numerical derivative of the reciprocal Green's functions of equation (7):

$$u_i(\mathbf{x},\ \mathbf{x}',\ t\ -\ t')\ =\ \frac{d\overline{G}_{ji}(\mathbf{x}',\ \mathbf{x},\ t\ -\ t')}{dx'_k}\ *\ M_{jk}(x',\ t') \quad (8)$$

Equations (7) and (8) allow us to evaluate a response due an arbitrary point source (double-couple, single-couple, explosive, or single force) without using body force equivalent forces (Burridge and Knopoff, 1964; Graves, 1996).

Numerical Implementation for the Finite-Difference Method

For the problem of wave simulation in complex three-dimensionally heterogeneous medium, we propose to calculate reciprocal Green's functions by interchanging the source and receiver positions. This is done by a standard finite-difference algorithm with a source placed at the receiver position. The results are then postprocessed to generate the seismograms that would have been obtained if the source and receiver had not been interchanged. The efficiency of the reciprocal method comes with the fact that for each reciprocal simulation, a number of pseudoreceivers can be recorded. When the postprocessing reverses the source-receiver relationship, this translates to synthetic seismograms due to many sources recorded at the same receiver.

The finite-difference technique we used is a velocity-stress equation solved by a staggered grid scheme (Virieux, 1984; Graves, 1996). For the receivers not situated on the free surface, no special treatment is necessary for the reciprocal calculations. However, if the receiver is situated directly on the free surface, a more careful implementation of the three orthogonal point forces is necessary. We empirically found the reciprocity is best satisfied by horizontal body forces implemented right at the free surface boundary and vertical force half a grid point below the free surface. This fits better than averaging over the two staggered vertical components above and below the surface. Equation (8) can be evaluated as recorded response to the three orthogonal point forces sources at the receiver site. This is simple for implementation in the finite-difference calculation since the response for the whole model for each time step is evaluated. To get $G_{ij,k}$ we can use numerical spatial derivatives of the displacement centered at the source locations. Either the numerical derivatives or the corresponding $\overline{G}_{ij}$ itself can be saved at each pseudosource point. One advantage of saving the $\overline{G}_{ij}$ comes if the source position is not known precisely and we would like to perturb its location. To save storage space we may store only certain products of the $\overline{G}_{ij,k}$. For example, if we are interested in the explosive sources, we only need to store $\overline{G}_{i1,1}$, $\overline{G}_{i2,2}$, $\overline{G}_{i3,3}$, or if we are interested in pure double-couple sources, we only need $\overline{G}_{i1,1}$, $\overline{G}_{i2,2}$, $\overline{G}_{i1,2}\ +\ \overline{G}_{i2,1}$, $\overline{G}_{i1,3}\ +\ \overline{G}_{i3,1}$, $\overline{G}_{i2,3}\ +\ \overline{G}_{i3,2}$.

One issue that arises in the practical application of the reciprocity method is that the boundary conditions are not completely reciprocal for finite-difference modeling. The most common boundary conditions used in finite-difference modeling are the free surface and absorbing boundaries. Free surface boundary condition satisfies in theory the condition of reciprocity relation (7) however, different finite-difference formulations of free surface boundary suffer various degree of inaccuracy (Zahradník *et al.,* 1993; or Graves, 1996). Discrepancies between direct and reciprocal seismograms can be used as a criteria for accuracy of the free surface boundary condition as has been suggested by Dellinger (1997). An absorbing boundary satisfies reciprocity to the extent that it mimics perfectly the unbounded homogeneous space. Imperfections in the numerical implementation of the different versions of absorbing boundaries do not in general satisfy the reciprocity. In the examples we show, we generally try to avoid any contamination of our seismograms with reflections from absorbing boundaries.

The Numerical Test

The reciprocal method can be tested by showing that identical seismograms can be obtained comparing standard forward calculations with reciprocal ones. We apply this test to synthetic seismograms computed for the three cases: an unbounded homogeneous medium, a case with a 1D variation of the medium parameters and a free surface, and a case with a 3D variation of the medium parameters. In each case, the results are computed with spatially fourth-order staggered-grid finite-difference scheme and second-order time derivatives. The finite-difference parameters are chosen to provide a reasonable level of modeling accuracy without prohibitive cost. The absorbing boundary conditions are the A1 of Clayton and Engquist (1977) and additional attenuating zone to minimize the artificial reflections.

Homogeneous Unbounded Medium

Figure 1 shows all nine components of the direct and reciprocal Green's functions $\overline{G}_{ij}(\mathbf{x},\ \mathbf{x}',\ t\ -\ t'$ and G_{ij} $(\mathbf{x},\ \mathbf{x}',$

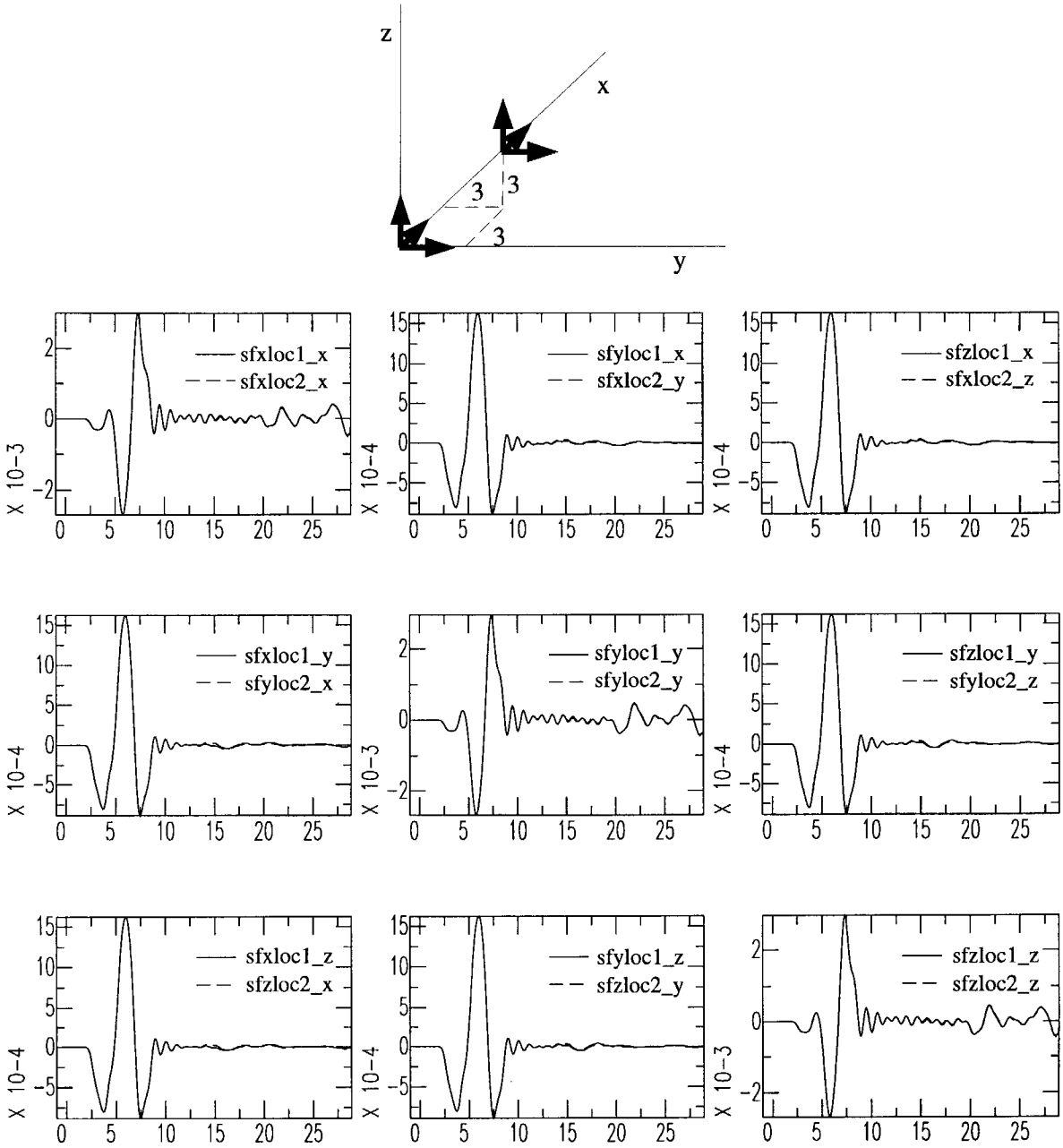

Figure 1. Nine pairs of Green functions $\bar{G}_{ij}(\mathbf{x}, \mathbf{x}', t - t')$ and G_{ij} $(\mathbf{x}, \mathbf{x}', t - t')$: loc1 (solid line) represents source at 0.0 km, 0.0 km, and 0.0 km and receiver at 3.0 km, 3.0 km, and 3.0 km, loc2 (dashed line) represents source at 3.0 km, 3.0 km, and 3.0 km and receiver at 0.0 km, 0.0 km, and 0.0 km. The first three letters denote the seismogram represent source type: six is single force into x direction, sfy is single force into y direction, and sfz is single force into z direction. The last letter denotes component at the receiver. The unbounded homogeneous medium was chosen with $\alpha = 2.0$ km/sec, $\beta = 1.0$ km/sec, and $\rho = 2.6$ g/m^3. Absorbing boundaries were placed at 12.0 km from the origin (0.0 km, 0.0 km, and 0.0 km).

$t - t'$) for homogeneous unbounded medium computed with the staggered-grid finite difference. The finite-difference results are accurate only for periods longer than 3 sec, however, we present unfiltered seismograms to demonstrate the reciprocity of not only the direct signal but also of the numerical noise generated by the finite-difference method. We can see the reciprocal pairs match within the thickness of the line. The solutions start to diverge slightly for time around 13–18 sec, which corresponds to the artificially reflected waves from boundaries. The nonreciprocal mismatch

increases with proximity to the absorbing boundary (as the waves hit boundary under more nonnormal incidence) and are caused by both *P* and S wave reflected from the boundary.

Free Surface and 1D Heterogeneous Medium

Figure 2 shows three components of the direct and reciprocal seismograms recorded in the vicinity of the free surface from a source at free surface. The 1D model and the source mechanism are described in the caption. The 1D structure traps energy in the upper layer of the model. Small discrepancies between the direct and reciprocal solution appear with the first arriving energy when the synthetic seismograms are computed with coarse sampling (five points per wavelength). These discrepancies are caused by inaccuracies in the implementation of the free surface boundary condition not exactly satisfying the continuity of the normal traction. The discrepancy diminishes as more accurate results are compared (right column with 7.5 points per *S*-wave wavelength in the top layer). Also note the slightly smaller amplitude computed with the finer grid; the more accurate computation evaluates more precisely the surface wave (which has a shorter wavelength than direct shear wave and therefore was computed with even less points per wavelength). This phenomena demonstrates the error due to the numerical implementation of the reciprocity (single force source at the free surface and numerical derivatives of the Green's functions) is smaller than error due to the finite-difference computation (i.e., accuracy of the scheme, free surface boundary condition accuracy, and absorbing boundaries).

Laterally Heterogeneous Medium

Figure 3 shows three pairs of components of a reciprocal and direct computation in strongly heterogeneous media. The 3D model and the source mechanism are described in the Figure 3 caption. We have simulated response due to a

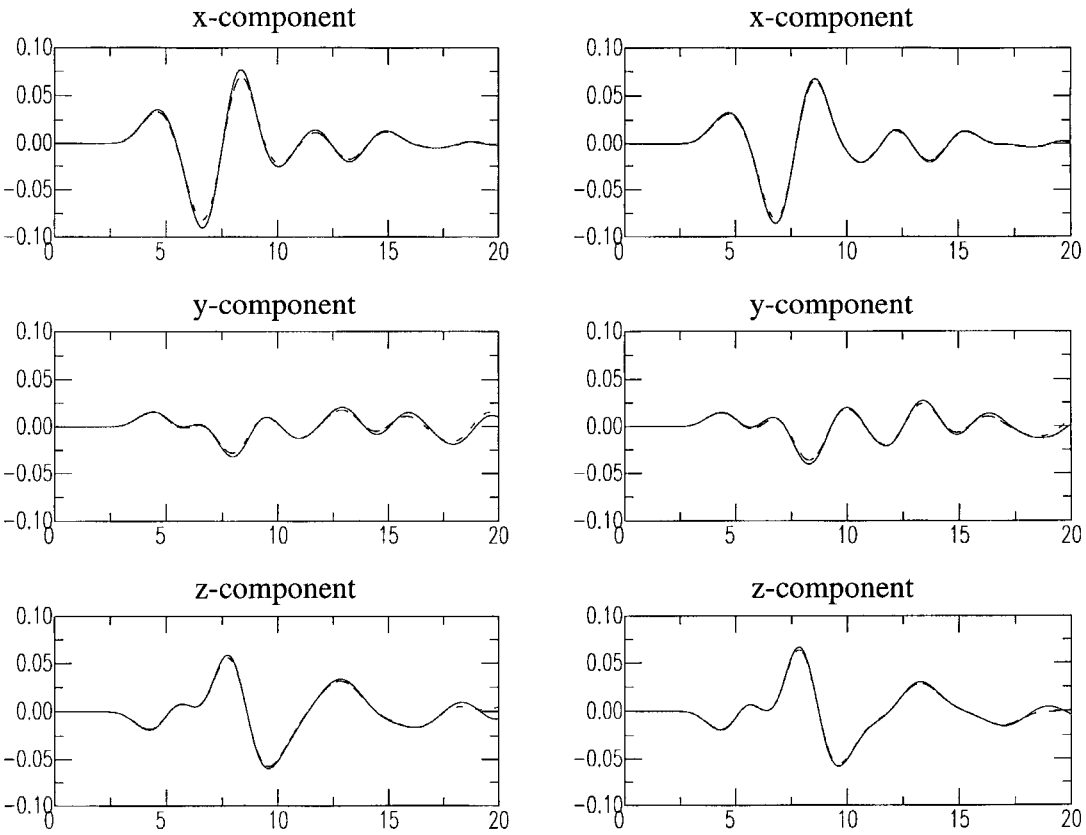

Figure 2. Three pairs of components of the acceleration (in mm/sec^2) due to double-couple source at 0.0 km, 0.0 km, and 3.6 km recorded at receiver 3.0 km, 3.0 km, and 0.0 km. The seismograms correspond to an earthquake of magnitude 1.0 with dip-slip (strike 0°, rake 90° and dip 90°); *x* axis is positive to the north, *y* axis is positive to the east and *z* axis is positive down. Solid line represents direct computation. Dashed line represents reciprocal computation. Left column was computed with five grid points per wavelength right column of seismograms was computed with 7.5 points per wavelength. Seismograms recorded in 1D heterogeneous medium with parameters: α = 2.0 km/sec, β = 1.0 km/sec ρ = 2.0 g/m^3 from surface to 3.0 km depth; α = 4.0 km/sec, β = 2.0 km/sec ρ = 2.3 g/m^3 from 3.0 km to 6.6 km depth; and α = 6.0 km/sec, β = 4.0 km/sec ρ = 2.7 g/m^3 from 6.6 km and deeper.

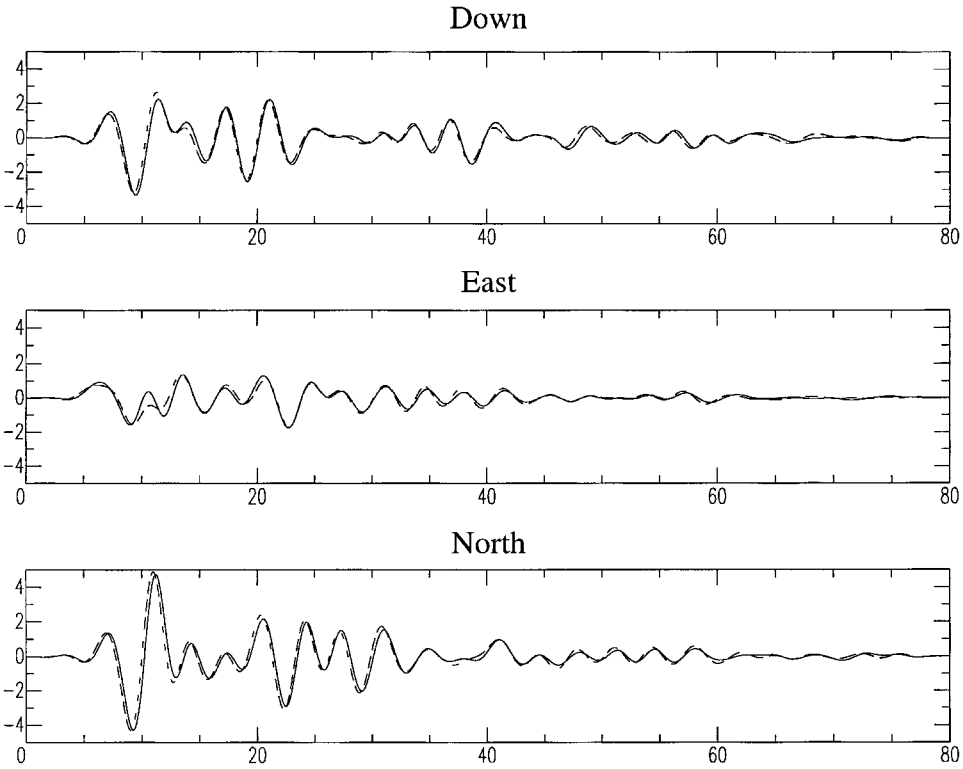

Figure 3. Three pairs of components of acceleration (in μm/sec^2) due to a double-couple source in laterally heterogeneous velocity model of Southern California SCEC version 1 (Magistrate *et al.* [1996]). The event simulates an aftershock of the Northridge earthquake (34.24°N, 118.47°W and depth z = 15.1 km) as recorded at Pasadena station (34.14°N, 118.17°W). The mechanism for point source double-couple of the aftershock is strike 109°, dip 63°, and rake 82° with magnitude 4.0 (coordinate system as that of Fig. 2. The velocity model includes strong lateral variations of both *P*- and *S*-wave velocities as well as densities due to the presence of the deep basins (Los Angeles and San Fernando in this case). The solid line represents the direct solution. The dashed line is a reciprocal seismogram recorded the free surface.

small earthquake in strongly heterogeneous medium. There are many arrivals caused by diffracted energy trapped in the sedimentary basin. Overall, we can see the fit is very good and direct calculation may be replaced with the reciprocal simulation. The discrepancy on the east component around 10 sec is caused by an artificial reflection from a model boundary that was close to the deep source used in the model. Note the largest discrepancies are on the smallest component.

Sampling of the Green's Functions in Heterogeneous Medium

Finally we would like to test the most efficient way of storing the derivatives of the Green's functions $\overline{G}_{ij}$ used for more complex sources suitable for iterative implementation of equation (8). We wanted to test if Green's functions $\overline{G}_{ij}$ can be stored instead of derivatives of the Green's function $\overline{G}_{ij,k}$. This way we hoped to be able to store Green's functions $\overline{G}_{ij}$ on coarse grid and reevaluate the derivatives of Green's functions $\overline{G}_{ij,k}$ in the postprocessing where needed. However, we show the accuracy of such an approach is not satisfactory.

Figure 4 shows three components of the two approximations of the seismograms due to single couple. The two approximations differ in the accuracy of evaluation of the $\overline{G}_{ij,k}(\mathbf{x}, \mathbf{x}', t-t')$ of equation (8). The solid line (same as in Fig. 2) represents numerical derivative of the second order over the smallest possible grid step (1/5 of the shortest wavelength of the *S* wave), the same as used in the finite-difference run. The dashed line was calculated from the second-order numerical derivative over the three grid steps (1.8 km). We can see the dashed line does not match the more accurate calculation both in amplitude (all components) and in phase. We have tested only second-order derivative of the Green's function as we compare with a direct solution evaluated with the second-order approximation of the moment tensor (Graves, 1996). Therefore, we need to directly store derivatives of the Green functions $\overline{G}_{ij,k}$ evaluated on a fine grid.

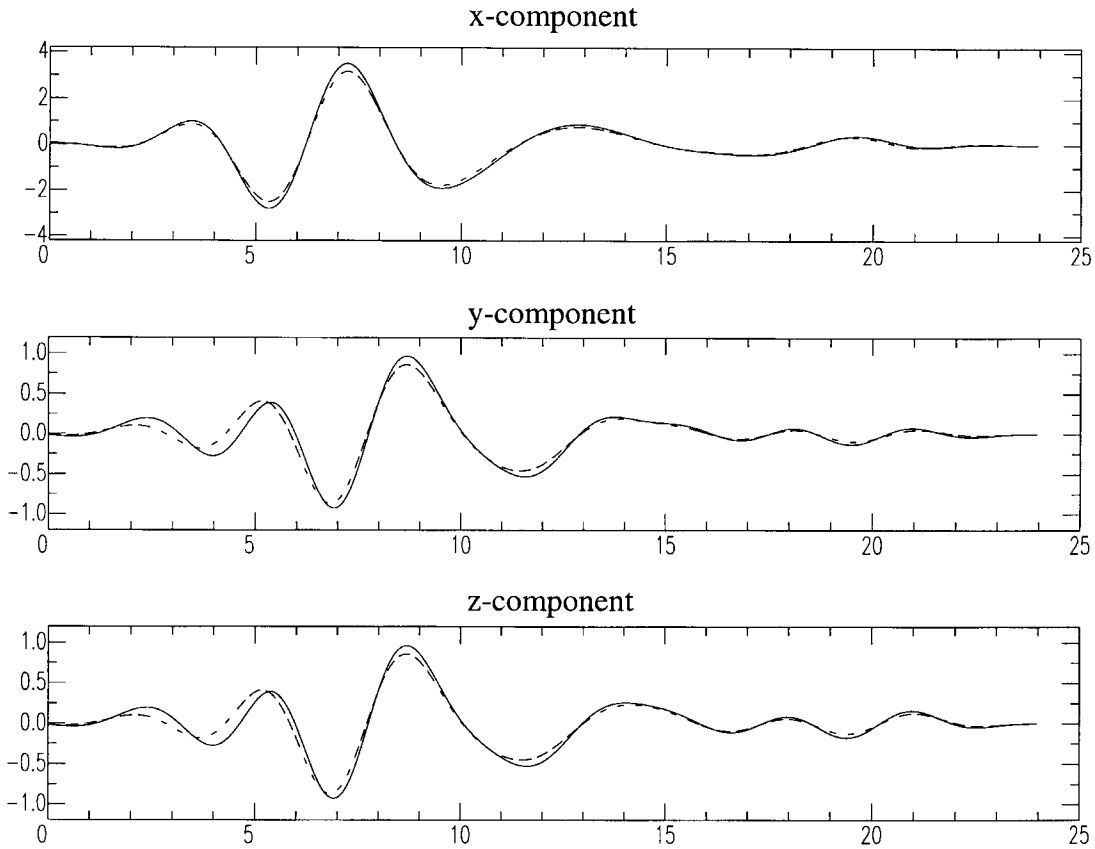

Figure 4. Three pairs of components of the acceleration due to single-couple source at 0.0 km, 0.0 km, and 2.6 km recorded at receiver 3.0 km, 3.0 km, and 0.0 km. Only component M_{zz} of the single couple was excited. Solid line represents the reciprocal computation from numerical derivatives of the Green's functions with spacing 0.6 km. Dashed line represents the reciprocal computation from numerical derivatives of the Green's functions with spacing 1.8 km. Seismograms recorded in 1D heterogeneous medium parameters as that of Figure 2.

Conclusions

The reciprocal method can be used to save a significant amount of calculations where seismograms from many sources at a few receivers are desired. The numerical tests show that the errors due to the numerical implementation of reciprocity method itself are less than the errors of the finite-difference method. The accuracy of the procedure is dependent upon calculation of the derivatives of the Green's functions to the same level of accuracy as the finite difference itself. The method is suitable for source inversion and source relocation, where large number of sources at different locations and with arbitrary mechanism can be quickly simulated. Another application is in determining the anticipated size of strong ground motions at particular site due to an earthquake at many locations.

Acknowledgments

The authors would like to thank Robert Graves for his input and the two reviewers Martijn de Hoop and Jiří Zahradník for their valuable suggestions. This research was supported by the Southern California Earthquake Center (NSF EAR-8920136 and USGS 14-08-0001-A0899 and 1434-HQ-97AG01718). The SCEC Contribution Number is 523.

References

Aki, K., and P. Richards (1980). In *Quantitative Seismology,* D. Johnson (Editor), W.H. Freeman, New York.

Bouchon, M., (1976). Teleseismic body wave radiation from a seismic source in layered medium, *J. Geophys. Res.* **47,** 515–530.

Burridge, R., and L. Knopoff (1976). Body force equivalents for seismic dislocations, *Bull. Seism. Soc. Am.* **54,** 1875–1888.

Červený, V. (2001). Seismic Ray Theory, Cambridge University Press, New York (in press).

Chapman, C. (1994). Reflection/transmission coefficient reciprocities in anisotropic media, *Geophys. J. Int.* **116,** 498–501.

Claerbout, J. (1976). Fundamentals of Geophysical Data Processing, McGraw-Hill, New York.

Clayton, R. W., and B. Engquist (1977). Absorbing boundary conditions for acoustic and elastic wave equations, *Bull. Seism. Soc. Am.* **67,** 1529–1540.

Dahlen, F., and J. Tromp (1998). *Theoretical Global Seismology,* Princeton University Press, Princeton, New Jersey.

de Hoop, M., and A. de Hoop (2000). Wave-field reciprocity and optimalization in remote sensing, *Proc. R. Soc. Lond. A* **456,** 641–682.

Dellinger, J. (1997). A crossed-dipole reciprocity "paradox," *Leading Edge* **16,** 1465–1471.

Graves, R. (1996). Simulating seismic wave propagation in 3D elastic media using staggered-grid finite differences, *Bull. Seism. Soc. Am.* **86,** 1091–1106.

Graves, R., and D. Wald (2001). Resolution analysis of finite fault source inversion using 1D and 3D Green's functions. I. Strong motions, *J. Geophys. Res.* (in press).

Graves, R. W. (1995). Preliminary analysis of long-period basin response in the Los Angeles region from the 1994 Northridge earthquake, *Geophys. Res. Lett.* **22,** 101–104.

Graves, R. W., and R. Clayton (1992). Modeling path effects in 3-dimensional basin structures, *Bull. Seism. Soc. Am.* **82,** 81–103.

Magistrale, H., K. McLaughlin, and S. Day (1996). A geology-based 3d velocity model of the Los Angeles basin sediments, *Bull. Seism. Soc. Am.* **86,** 1161–1166 (*http://www.scecdc.scec.org/3Dvelocity/3Dvelocity.html*).

Olsen, K., R. Madariaga, and R. Archuleta (1997). Three-dimensional dynamic simulation of the 1992 Landers earthquake, *Science* **278,** 834–838.

Virieux, J. (1984). SH wave propagation in heterogeneous media: velocity-stress finite-difference method, *Geophysics* **49,** 1933–1957.

Wald, D., and R. Graves (1998). The seismic response of the Los Angeles basin, California, *Bull. Seism. Soc. Am.* **88,** 337–356.

Zahradnik, J., P. Moczo, and F. Hron (1993). Testing four elastic finite-difference schemes for behavior at discontinuities, *Bull. Seism. Soc. Am.* **83,** 107–129.

Seismological Laboratory
California Institute of Technology
Pasadena, California
eisne@gps.caltech.edu

Manuscript received June 2000.